Indian Journal of Chemical Technology
Vol. 30, May 2023, pp. 370-378
DOI: 10.56042/ijct.v30i3.68031

Comparison study of COD adsorption on bentonite-based nanocomposite materials in landfill leachate treatment: Characterization, Isotherms, Kinetics and Regeneration

Hajjizadeh Matin[1], Goodarzvand Chegini Zahra[2], Mehralian Mohammad[3] & Khashij Maryam*[,4]

[1]Department of Environmental Science, Faculty of Natural Resources and Environment, Science and Research Branch, Islamic Azad University, Tehran, Iran

[2]Department of Environmental Science, Faculty of Natural Resources and Environment, Science and Research Branch, Islamic Azad University, Tehran, Iran.

[3]Environmental Science and Technology Research Center, Department of Environmental Health Engineering, School of Public Health, Shahid Sadoughi University of Medical Sciences, Yazd, Iran.

[4]Environmental Science and Technology Research Center, Department of Environmental Health Engineering, School of Public Health, Shahid Sadoughi University of Medical Sciences, Yazd, Iran.

E-mail: m.khashij@yahoo.com

Received 28 October 2022; accepted 3 April 2023

The COD removal from landfill leachate using bentonite-based nanocomposites prepared using different modifiers has been investigated. Different techniques including FE-SEM, XRD, FTIR, TGA and Zeta potential have been utilized for characterization of nanocomposites (NCs). The independent variables includingNCs dose, *p*H and contact time are studied for COD removal efficiency. The optimal values are obtained to be a NCs dose of 40 g/L, pH of 3.00, and a contact time of 20 min for maximized COD removal efficiencies of 67.90, 71.30 and 52.00% using Arg/CTS-BEN, H/CTS-BEN and CTS-BEN NCs, respectively. Kinetics studies fitted well with the pseudo-second order model with rate constants of 25.64, 28.65 and 25.00 mg/g by H/CTS-BEN, Arg/CTS-BEN and CTS-BEN NCs, respectively. The adsorption of the COD is well described by Langmuir equations (R^2 0.99). Results show that the synthesized NCs is promising and efficient in purifying landfill leachate.

Keywords: Bentonite-based nanocomposite, COD, Leachate, Regeneration

Leachate is a by-product derived from the decomposition municipal solid wastes, which not only pollutes the water resources but also it causes soil pollution[1]. Treatment of municipal landfill leachate is essential concern due to contamination such as organic (COD and BOD_5), inorganic matters (NH_4-N and NO_3-N), and potentially heavy metals to protect of groundwater and surface waters[2]. This issue has increased the need for the development of new strategies to deal with pollution to have an adequate water supply and confirm the sustainability of clean water resources[3]. All treatment approaches can be performed as physical, chemical, and biological process. Typically, different types of these methods are (i) physical processes such as filtration with membrane technologies, sedimentation, and adsorption[4,5]; (ii) chemical processes like ion exchange, advanced oxidation process (AOPs), coagulation, electrochemical, and catalytic reduction[6,7]; (iii) biological processes such as biodegradation, wetlands, phytoremediation, and bioreactor processes[8-10]. These procedures have advantages and disadvantages, and they usually require high capital and operational cost[3]. Adsorption, as one of the promising methods, has been constantly employed in the removal of different contaminants. This procedure removes a wide range of contaminants by mass transfer process on the internal or external solid surfaces[2]. Natural and synthetic adsorbents are used to separate the impurities in the adsorption process[11]. Clay minerals and composite materials are a very interesting platform for the synthesis of novel adsorbents[12]. Although technological innovations are constant proposed for leachate treatment, the adsorption approach is still noticed. It is cost-efficient and relatively inexpensive to reduce contaminants from polluted environments. Surface modifications of clay-based adsorbents have received attention because they lead to the synthesis of new compounds and, following, the expansion of new applications.

Modification of clay minerals with organic compounds has been demonstrated to be a practical step for their industrial applications, such as for synthesis of clay-based nanocomposites[13, 14]. The organic modification can promote compatibility between organic and inorganic phases and improve interfacial interactions between them[15]. Bentonite are highly significant owing to their high surface area, mechanical strength, chemical stability, satisfactory cation exchange capacity (CEC) and availability, particularly in Iranian soil[16]. However, bentonite does not have a sufficient adsorption capacity for uptake contaminants because of poor interaction with some polar adsorbate. This causes many researchers have been focused on modifying the bentonite or producing composite adsorbents with high capacity to interact between polar or non-polar adsorbates. Several studies illustrated different modifications of bentonite for the formation of nanocomposites with remarkable results. Resende *et al*. modified bentonite with the surfactant CTAB and used it for the removal of fatty acids with excellent capacity[17]. Recently, Marszałek *et al*. showed noteworthy contributions regarding carbon nanotubes modification on bentonite at various reaction temperatures. Synthesized nanocomposite showed over 90% simultaneous reduction of anthracene, benzotriazole, Zn^{2+}, and Pb^{2+}[18]. Various modifiers lead to the synthesis of nanocomposites with different adsorption capacities. Thus, this study aims to compare landfill leachate treatment in terms of COD removal using three nanocomposites synthesized with the various modifiers (Surfactant, Amino acid, and Biopolymer). Nanocomposites were characterized using FE-SEM, XRD, FTIR, TGA, and Zeta potential analysis. Besides, kinetic and isotherm modelling and regeneration studies were investigated.

Experimental Section

Chemicals

In the current study, Bentonite with 40 meq/100 g of CEC was used from the Aavaj mine (Khoros Dareh village, Qazvin). L-Arginine ($C_6H_{14}N_4O_2$, 99%), Hexadecyltrimethylammonium bromid (CTAB,$CH_3(CH_2)_{15}N(Br)(CH_3)_3$, ≥98%), Chitosan ($C_{56}H_{103}N_9O_{39}$) were purchased from Sigma-Aldrich company (Germany). Dilute HCl and NaOH (0.1 M) were utilized for adjustment of *p*H. All solutions were prepared with deionized water.

Landfill leachate

Leachate samples were collected from Mohammadabad landfill site that is situated at 25 km south of Qazvin. This landfill covers an area of about 110 ha, and it receives 750 t of solid waste daily. Samples were collected from the evaporated ponds with a 20 L plastic container, transported to the laboratory, and held at 4°C. Leachate characteristics are detailed in supplementary data.

Preparation of H/CTS-BEN, Arg/CTS-BEN, and CTS-BEN nanocomposites

H/CTS-BEN nanocomposite

To preparation of H/CTS-BEN nanocomposite, 30 g of the bentonite in deionized water was dispersed for 30 min at 250 rpm. The HDTMA-Br solution (1 g CTAB in 100 mL solution) was slowly added to the bentonite mixture. The suspension of bentonite and HDTMA-Br were stirred for 4 h and separated through a vacuum filtration system. The CTAB-B suspension was washed with deionized waterand then dried in an oven at 65°C for 12 h. Next, chitosan (CTS) was dissolved in 0.7 M acetic acid and mixed on the magnetic stirrer at 60 C for 30 min. The resulting solution was added dropwise to the CTAB-B suspension. This reaction was performed for 4 h at 60°C. The prepared nanocomposite was washed several times with deionized water and labeled H/CTS-BEN nanocomposite.

Arg/CTS-BEN nanocomposite

To synthesis of the Arg/CTS-BEN nanocomposite, 30 g of raw bentonite in deionized water was stirred for 30 min. A stoichiometric amount of the L-Arginine (Arg) was poured into deionized water and its *p*H was adjusted to 3 with 0.1 M HCl. The L-Arginine solution was slowly added to the bentonite and mixed using a stirrer for 4 h at 60°C. The chitosan prepared in the aforementioned step (2.3.1) was slowly added to the Arg-BEN suspension. Reaction between the Arg-BEN suspension and CTS was performed for 4 h at 60 °C under acidic condition. Precipitates were washed several times and labeled Arg/CTS-BEN nanocomposite.

CTS-BEN nanocomposite

To compare the effect of chitosan alone on bentonite modification, a CTS-BEN nanocomposite was prepared with 4 wt% of bentonite. The ion exchange method was utilized to CTS-BEN nanocomposite preparation. The CTS-BEN synthesis

method was similar to the Arg/CTS-BEN and H/CTS-BEN nanocomposites without the addition of surfactant and amino acids. Chitosan (4 wt%) was dissolved in 0.7 M acetic acid and mixed at 60°C for 30 min to protonate its NH_2 groups. Then the CTS solution was slowly added to the BEN suspension.After a time, the CTS-BEN nanocomposite was washed, dried, and placed in a plastic container.

Measurement and Characterizations

All nanocomposites synthesized were characterized by FE-SEM (MIRA3TESCAN-XMU), FTIR in a wavelength range of 400–4000 cm^{-1}(Perkin-Elmer spectrometer, BX spectrum, USA), XRD (X-ray Diffractometer Panalytical.s X.Pert Pro), TGA (TA Instruments DSC SDT Q600), and Zeta potential. The concentration of COD and adsorption capacity was determined using Eqs. 1-2.

$$R(\%) = \frac{C_i - C_e}{C_i} \times 100 \quad \ldots(1)$$

$$q_e = \frac{(C_i - C_e)}{m} \times V \quad \ldots(2)$$

where R (%) was the COD adsorption efficiency, C_i (mg/L) was the initial concentration of contaminants, C_e (mg/L) was the concentration of contaminants at time t, q_e (mg/g) was the adsorbed amount at time t, m (g) was the nanocomposite dosage, and V (L) was the volume of solutions.

Adsorption studies

Adsorption experiments were conducted on the COD adsorption onto the synthesized nanocomposites. The influence of different variables such as dose of nanocomposites, contact time and *p*H were investigated. Adsorption tests were carried out in the *p*H range between 2-11 concerning COD and turbidity. The dose of nanocomposite for COD adsorption was used at 10-70 g/L. Also, the variation of contact time ranging from 10 to 100 min was considered for adsorption efficiency.

Isotherm and kinetic modelling

For configuration purposes, the relationship between equilibrium concentrations (C_e) and adsorption efficiency (q_e) was analysed using Langmuir, Freundlich, and Temkin isotherm models. The kinetic investigations provide valuable information with regard to adsorption rate of contaminants, which associated with adsorption mechanism. The kinetic data was analysed by Pseudo -first order, Pseudo -second order, and Elovich kinetic models.

Desorption with regeneration

Desorption was conducted using 0.1M of HCl and NaOH for several sorption-desorption cycles.

Results and Discussion

Characterizations

FE-SEM

FE-SEM images of synthesized NCs are presented in Fig. 1 (a-d). Based on FE-SEM image, an irregular flake and massive structure is clearly seen for raw BEN [Fig. 1 (a)]. After modification with L-Arginine, the Arg/CTS-BEN nanocomposite was less aggregated and had larger and more numerous flakes [Fig. 1 (b)]. Enhanced adsorption capacity is caused by fragmentation of the flakes due to modification process of nanocomposites[19]. Due to the hydrophilicity of the raw BEN and the hydrophobicity of the HDTMA-Br, a strong repulsion occurs between the functional groups. In this case, the HDTMA-Br and CTS increase the basal space and create a coarse flake morphological structure [Fig. 1 (c)]. This causes the nanocomposite morphology to be significantly affected by tension-induced rupture after modification[20]. Fig. 1(d) demonstrates clearly the exfoliation of raw BEN in a CTS matrix, thus confirming the formation of intercalated nanocomposite, leading to the exfoliation of raw BEN. Uniformly dispersed small particles have been achieved compared to the raw BEN. This may be due to the Na^+ ions in the raw BEN can be exchanged for modifying agents[21].

FTIR

The infrared spectrum of the synthesized nanocomposites in the region from 4000-400 cm^{-1} is presented in Fig. 2. The typical adsorption band at 1028.79 cm^{-1} that is related to asymmetric bridge bonds Si-O...Si of raw BEN, appeared in the curve of CST-BEN NCs, demonstrating the silicate layer structure of BEN was not changed after the reaction of CTS with BEN. In the CTS-BEN, the hydrogen stretching vibration band at 3625 cm^{-1} in the curve of raw Arg/CTS-BEN disappeared. Other hydroxyl-related infrared absorption bands at 3401.58 (-OH), 1028.79 (Al-OH), and 793.63 cm^{-1} (Al-Mg-OH) were also increased or altered[22, 23]. The

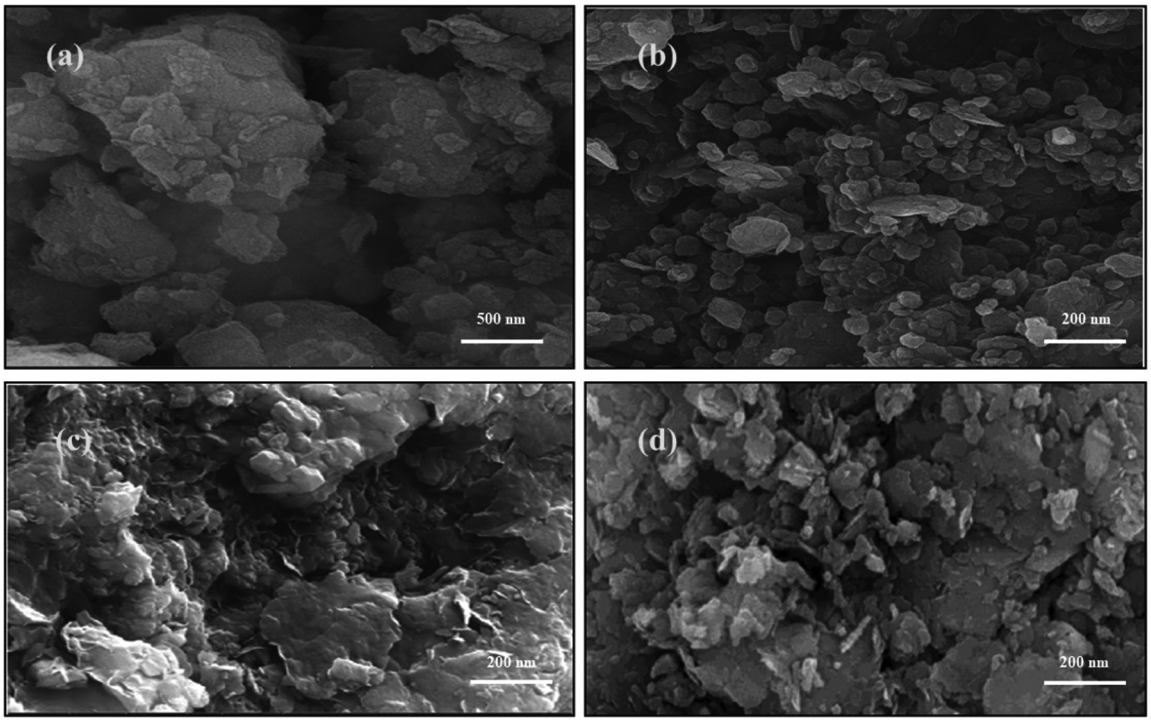

Fig. 1 — FE-SEM images of synthesized NCs. (a) Raw BEN; (b) Arg/CTS-BEN; (c) H/CTS-BEN and (d) CTS-BEN NCs.

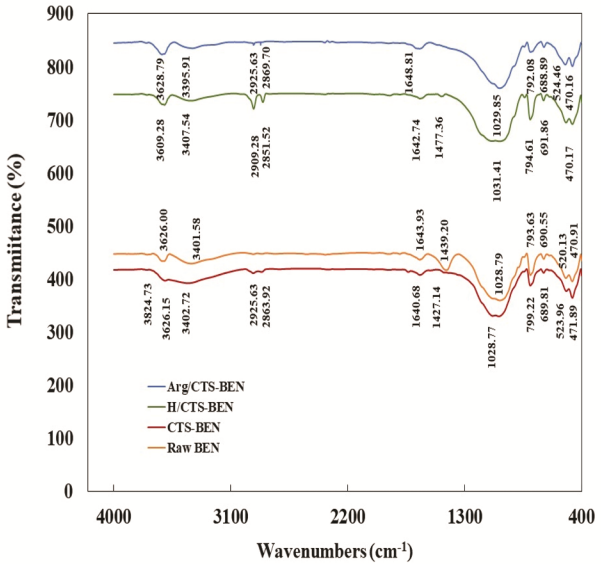

Fig. 2 — FTIR patterns of raw BEN, Arg/CTS-BEN, H/CTS-BEN and CTS-BEN NCs.

typical band of CTS assigned to NH_2 groups at 1427.14 cm^{-1} was also disappeared due to reaction between amino groups on CTS with OH groups on the raw BEN[24]. The band at 3626.00 cm^{-1} in raw BEN is assigned to the hydroxyl structural group. This peak is transferred to 3609.26 cm^{-1} with modification of BEN with the HDTM-Br, indicating the new hydrophobic behaviour of the H/CTS-BEN NCs. Modification of BEN with HDTM-Br increased the intensity at around 2851.59 and 2909.28 cm^{-1} that associated with asymmetric and symmetric stretching of the CH_2 groups[25]. Based on Fig. 2, the -OH groups at 3626.00 cm^{-1} position in raw BEN sample is changed after modification with L-Arginine. This change might be due to the replacing the water molecules by amino acid (L-Arginine) in the internal space of clay[26]. The band at 1648.81cm^{-1} is related to the existence of L-Arginine in the Arg/CTS-BEN nanocomposite. The carboxylic stretch C=O of an L-Arginine appears at this band. Formation of hydrogen bond between the side-chain-amino group and thecarboxylic acid in the Arg/CTS-BEN nanocomposite lead to this phenomenon. Results prove the L-Arginine can hide the negative charge of carboxylic acid via intermolecular hydrogen bond[27]. FTIR patterns described the presence of a robust affinity between modifiers (HDTM-Br and L-Arginine) with an interlayer space of BEN, and thus lead to the formation of a new substance. This phenomenon causes the various structures of the clays and the monomers will show different properties[28].

XRD

The XRD pattern of synthesized nanocomposites are compared in Fig. 3. The XRD patterns present that the raw BEN contains a 26.69 Å mineral quartz, illite,

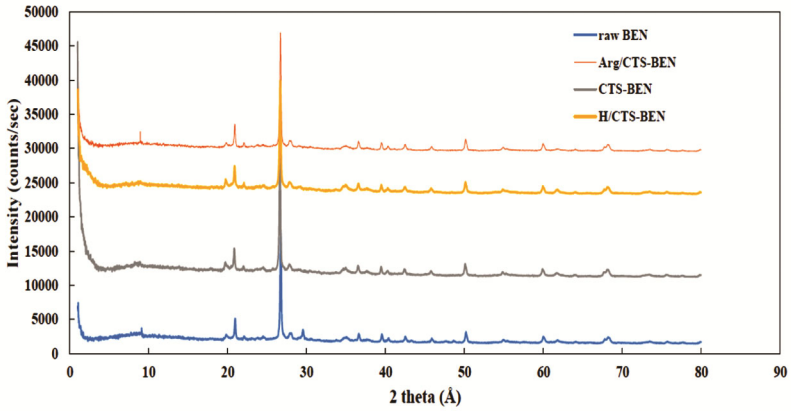

Fig. 3— XRD pattern of synthesized nanocomposites at 2 theta (Å).

calcite, and albite. For the raw BEN, an intensity about 9.79 Å shifts to 10.15 Å after modification with amino acid. These results confirm that the successful loading of L-Arginine in the interlayer space of bentonite[29]. In CTS-BEN nanocomposite, the peak at 10° vanished due to the break of the neutral or ionic intermolecular hydrogen bonds and the crystalline nature of chitosan, demonstrating prosperous modification of chitosan with raw BEN[30]. The intensity of CTS crystalline peak decreases from 21.9°to 21° for the CTS-BEN nanocomposite. These results indicate a decrease in the crystalline property of chitosan and a slight deformation of the silicate layers in the CTS-BEN nanocomposite[31]. The XRD pattern of the Arg/CTS-BEN and H/CTS-BEN NCs showed that functionalizing the raw BEN would not lead to a phase change. However, the extension of layers in the H/CTS-BEN nanocomposite is less than that of the Arg/CTS-BEN, and the interlayer spacing in the Arg/CTS-BEN is greater than in H/CTS-BEN nanocomposite. This can be attributed to the higher amino acid loading compared to the cationic surfactant.

TGA

Thermogravimetric analysis (TGA) of raw BEN, Arg/CTS-BEN, H/CTS-BEN, and CTS-BEN NCs are shown in supplementary data. The first step of mass loss (10–15%) at below 200°C is associated with the loss of interlayer water molecules. The continuous weight loss that corresponds to the dehydration of exchangeable cations, observed at temperature of 200-700°C (Second step).The third weight loss is due to the loss of hydroxyl groups at temperatures above 700°C[31]. Comparison of TGA curves of H/CTS-BEN [Fig. 4 (b)] with Arg/CTS-BEN show that the rate of weight loss in Arg/CTS-BEN is higher than H/CTS-BEN NCs. Weight loss in H/CTS-BEN and Arg/CTS-BEN NCs was 13.7% and 27.1%, respectively that is related to the higher concentration of amino acid loading than the cationic surfactant.

Zeta potential

The zeta potential of raw BEN gradually changed from negative (-31.4 mV) to positive (+10.3 mV and +1.5 mV) after modification process with L-arginine and cationic surfactant, respectively. In addition, CTS-BEN has a zeta potential of -13.7 mV. Indeed, the protonated eNH_2 groups on CTS leads to positively charged of CTS in acidic conditions that could be saturate of the negative charges on raw BEN. As the zeta potential changed from negative to positive with modification, the enhanced adsorption capacity should not be related to the electrostatic interaction or cation exchange; instead, the interactions between CTS and cation, i.e., cation binding to the CTS functional groups (e.g., eOH, eNH_2), could be the primary cause for the increased adsorption of cation on modified nanocomposites[32].

Batch adsorption experiments

Effect of pH

Solution *p*H as a crucial parameter is considered for adsorption of contaminants. All organic matters with proton binding sites can exist in cationic, anionic, and neutral form depending on the solution *p*H[33]. Therefore, influence of *p*H on adsorption rate was investigated which is shown in Fig. 4. The maximum COD adsorption was obtained in acidic condition (*p*H 3).Comparison of removal efficiency with all three nanocomposites showed that H/CTS-BEN and CTS-BEN NCs caused the highest and

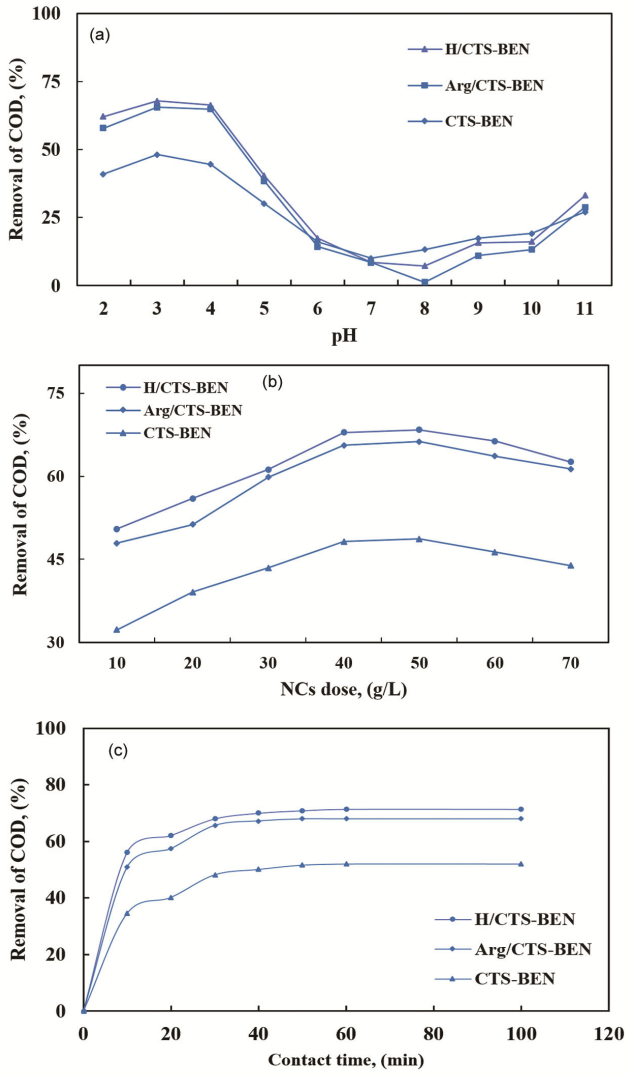

Fig. 4 — (a) Effect of contact time on COD removal by different nanocomposites at 25°C; (b) Effect of initial *p*H on the COD adsorption onto various nanocomposites. Contact time: 30 min, Nanocomposite dosage: 40 g/L, and Temperature: 25°C and (a) Effect of nanocomposite dosage on COD removal by different nanocomposites at 25°C.

lowest COD removal, respectively. The removal percentage of COD was 67.9, 65.5, and 48.2% by H/CTS-BEN, Arg/CTS-BEN, and CTS-BEN NCs, respectively. When the solution *p*H raised from 3.0 to 8.0, the removal percentage of COD due to the decreasing positive charge declined. In acidic *p*H, due to increase in H^+ and decrease in OH^- ions, cause the synthesized nanocomposites to have positive charge; thus, electrostatic attraction force between the nanocomposites and COD molecule, it can adsorb negatively charged species[34]. As the *p*H increases to 11.0, the removal of COD in all three nanocomposites increases but is less than in acidic conditions. Under alkaline conditions, the functional groups available on the bentonite surface are completely or partially deprotonated and lead to increase the negative charge on the nanocomposite surface. This phenomenon is due to the presence of -OH and COO- groups leading to increased electrostatic force between active sites and contaminant[35].

Effect of nanocomposite dosage

Nanocomposite dosage is one of the other effective factors in the adsorption process, which investigated in Fig. 4 (b). Comparison of results indicate that the H/CTS-BEN nanocomposite was the most effective for COD removal (68.4%). The results of nanocomposite dosage exhibit that by increasing the nanocomposite amount from 10 to 40 g the COD removal was enhanced, which is due to increase of available active sites number, which in turn improves the contact surface between the nanocomposite and contaminants. As shown in Fig. 4 (c), with increasing dosage from 10 to 40 g, an increase in percentage ratio from 50.5 to 67.9%, 47.9 to 65.5% and 32.3 to 48.2% was obtained for H/CTS-BEN, Arg/CTS-BEN, and CTS-BEN, respectively. Increasing the nanocomposite dose up to 50 g/L caused a slight increase in COD removal approximately 0.5, 0.8 and 0.6% for H/CTS-BEN, Arg/CTS-BEN, and CTS-BEN NCs, respectively. Based on cost-effectiveness of each process, the optimal dose of 40 g was selected for further investigation. There was no further increase in the COD removal at dosage from 50 to 70 g, which is associated with aggregation of active sites with excess dosage. This decrease in removal percentage has been related to increasing adsorption active sites leading in less utilization due to aggregation of the sites as explained earlier. These results are similar to those reported by many researchers for various contaminants[36-38].

Effect of contact time

One of the significant variables in COD removal by adsorption process is the contact time for interaction between the nanocomposite and COD molecules. In this study, contact time in the range between 10 to 100 min was studied for COD removal efficiency Fig. 4(c). COD removal percentage for H/CTS-BEN, Arg/CTS-BEN, and CTS-BEN NCs were obtained 71.3%, 67.9%, and 52%, respectively. The results presented in Fig. 4(c) demonstrate that at the beginning of the reaction due to existence of more

Table 1 — Kinetic and isotherm modelling comparison for COD removal.

		H/CTS-BEN	Arg/CTS-BEN	CTS-BEN
q_e (Exp)(mg/g)		9.47	8.33	9.88
Pseudo-first-order	q_e (mg/g)	6.22	3.53	4.90
	K_1(L/mg)	0.0645	0.0411	0.0508
	R^2	0.94	1.00	0.95
	RMSE	3.36	4.84	5.03
Pseudo-second-order	q_e (mg/g)	10.10	8.77	10.53
	K_2(L/mg)	0.01792	0.02166	0.01770
	R^2	0.99	1.00	0.99
	RMSE	0.34	0.20	0.39
Elovich	α	3.4016	3.7469	5.9128
	β	0.8264	0.9560	0.8547
	R^2	0.97	0.99	0.97
	RMSE	2.88	2.34	2.76
Langmuir	q_m (mg/g)	25.641	28.653	25.000
	K_L(L/mg)	0.217	0.048	0.714
	R_L	0.32-0.03	0.68-0.12	0.12-0.01
	R^2	0.99	0.999	0.987
	RMSE	0.908	0.094	2.830
Freundlich	K_f (L/mg)	4.665	1.649	9.3
	N	2.00	1.449	3.333
	R^2	0.95	0.973	0.980
	RMSE	2.329	1.847	1.126
Temkin	AT(L/g)	3.94	0.75	95.32
	bT	563.4	476.7	922.2
	B(J/mol)	4.4	5.2	2.688
	R^2	0.98	0.960	0.943
	RMSE	0.935	1.154	1.759

active sites number, COD removal efficiency raises at 20 min, the reaction reached its equilibrium limit (60 min), and elimination rate displayed no considerable difference from this moment on. This could be attributed to reduce in COD concentration as well as decrease in active sites number available on the nanocomposites surface[37].

Kinetics and isotherm modelling

The kinetics modelling were applied to determine multistep mechanisms adsorption processes[39]. Kinetic analysis was conducted with the pseudo first-order, pseudo-second-order, and Elovich equations. The kinetics modelling of COD removal with respect to the various contact times is shown in Supplementary data and the kinetic parameters are shown in Table 1. The R^2 values of H/CTS-BEN, Arg/CTS-BEN, and CTS-BEN NCs were observed to be 0.99, 1.00 and 0.99 for the pseudo-second-order kinetic model, respectively. The best correlation of the model fitting has the highest R^2 value. Among the synthesized nanocomposites, Arg/CTS-BEN shows a strong correlation (R^2=1) for the pseudo-second-order. Arg/CTS-BEN displayed the fastest adsorption rate followed by H/CTS-BEN and CTS-BEN NCs. Based on Table 1, experimental adsorbed amount of the COD ($q_{e.exp}$) are same to the calculated amounts ($q_{e.cal}$) from models. This may be related to that more COD molecules were immediately bounded on the nanocomposite surface due to the increased mass transfer rate. Similar result was reported by Gulen *et al.* in the adsorption of ciprofloxacin into dioctahedral clay[40]. Besides, many researchers were stated similar kinetics results for the adsorption kinetics of pollutants[41, 42]. Based on the assumption of pseudo-second-order kinetic model, the adsorption of COD onto nanocomposites is chemisorption. Chemical adsorption refers to electrostatic phenomenon due to ion exchange activity on the nanocomposite surface, while physical adsorption mostly takes place on the surface of non-polar pores. Due to the nature of organic molecules (polar and non-polar) and the CEC of nanocomposites, both physical and chemical adsorptions are proposed as the dominant adsorption mechanisms.

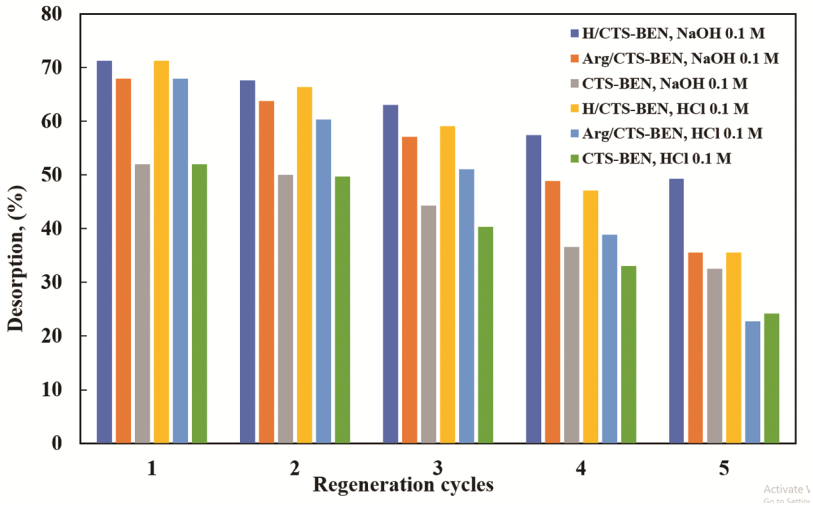

Fig. 5 — Reusability analysis of synthesized nanocomposites for the removal of COD.

On the other hand, Table 1 shows the comparisons of isotherm constants between H/CTS-BEN, Arg/CTS-BEN, and CTS-BEN NCs. To identify the adsorption mechanisms, the generally isotherm models such as Langmuir, Freundlich, and Temkin models were used to fit the equilibrium adsorption data (Refer to supplementary data). Langmuir isotherm model refers to the monolayer adsorption on a homogeneous surface, which is favourable where 0 $<R_L>1$. Unlike the Langmuir model, Freundlich isotherm describes the multilayer adsorption. n values of 1–10 as the heterogeneity factor represent that adsorption is favourable[43]. The R^2 values confirm the good correlation of the experimental data with the Langmuir model more than with two other models. The maximum capacity of COD were obtained using the Langmuir model at 28.65 mg/g for Arg/CTS-BEN nanocomposite (R^2 0.99). Similar isotherm results were reported by Ravi *et al.* for adsorption process[44]. This result reveals that monolayer adsorption occurs on a uniform nanocomposite surface with the same adsorption energy. In this state, the adsorption capacity with new active sites increases leading to a process does not involve a strong interaction between the adsorbate molecules.

Reusability

To evaluation of feasibility studies, the synthesized nanocomposites were reused several times. Fig. 5 demonstrated the five repeated desorption cycles with acid and base solution as desorbing agent for COD removal. The results indicated that NaOH was better eluent than HCl for the regeneration of studied nanocomposites. The sorption of COD with NaOH as eluent declined from 71.3 to 49.3%, 67.9 to 35.6%, and 52 to 32.5% concerning H/CTS-BEN, Arg/CTS-BEN and CTS/BEN NCs after five cycles, respectively (Fig. 5). Reduction in sorption rate using HCl 0.1 M reached 71.3 to 35.6%, 67.9 to 22.7%, and 52 to 24.1%, respectively. The reduction in COD sorption could be associated with the loss of nanocomposite mass and active sites caused by the eluent washing[45]. The results of reusability revealed that the synthesized nanocomposites could be efficiently regenerated up to fifth cycle with by NaOH treatment.

Conclusion

H/CTS-BEN, Arg/CTS-BEN and CTS-BEN NCs were studied as a natural, green and promising composite media for the removal of COD molecules from real landfill leachate. The nanocomposites were characterized using FE-SEM, XRD, FTIR, TGA and Zeta potential techniques. The optimized variables for maximum sorption were obtained as follows: *p*H (3), contact time (20 min), and NCs dosage (40 g/L). COD removal percentage for H/CTS-BEN, Arg/CTS-BEN, and CTS-BEN NCs were obtained 71.3%, 67.9%, and 52%, respectively at equilibrium time. The Zeta potential was increased after modification. The maximum monolayer sorption capacity of COD was obtained 25.64, 28.65 and 25.00 mg/g with H/CTS-BEN, Arg/CTS-BEN and CTS-BEN NCs, respectively. The isotherms comparison study showed that the adsorption of COD onto nanocomposites obeyed the Langmuir isotherm model (R^2 0.99). The best followed kinetic model was pseudo-second order model. Chemisorption as the dominant mechanism

was proposed for COD removal. The synthesized nanocomposites also display excellent reusability and can be regenerated successfully up to five cycles. It is concluded that the synthesized nanocomposites can be utilized to treat the leachate from landfill sites.

Declaration of Competing Interest

The authors declare that they have no conflict of interest.

Acknowledgements

The authors acknowledge Alborz Industrial City by providing the laboratory conditions.

References

1 Veli S, Arslan A, Isgoren M, Bingol D & Demiral D, *Environ Challenges*, 5 (2021) 100369.
2 Mohammad-Pajooh E, Turcios A E, Cuff G, Weichgrebe D, Rosenwinkel, K H, Vedenyapina, M D & Sharifullina L R, *J Environ Manag*, 228 (2018) 189.
3 Shadi A M H, Kamaruddin M A, Niza N M, Emmanuel M I, Ismail N & Hossain S, *J Water Process Eng*, 40 (2021) 101988.
4 Yang Y, Ricoveri A, Demeestere K & Van Hulle S, *J Hazard Mater*, 430 (2022) 128481.
5 Yuan Y, Liu J, Gao B & Hao J, *Sci Total Environ*, 794 (2021) 148557.
6 Mehralian M, Khashij M & Dalvand A, *Environ Sci Pollut Res*, 28 (2021) 45041.
7 Scandelai A P J, Zotesso J P, Jegatheesan V, Cardozo-Filho, L & Tavares C R G, *Waste Manag*, 101 (2020) 259.
8 Wdowczyk A, Szymańska-Pulikowska A & Gałka B, *Bioresour Technol*, 353 (2022) 127136.
9 Saxena V, Padhi S K, Dikshit P K & Pattanaik L, *Environ Nanotechnol Moniter Manag*, 18 (2022) 100689.
10 Mousavi S A, Mehralian M, Khashij M & Ibrahim S, *J Environ Technol*, 39 (2018) 2891.
11 Reshadi M A M, Bazargan A & McKay G, *Sci Total Environ*, 731 (2020) 138863.
12 Gil A, Santamaría S A, Korili M A, Vicente L V, Barbosa S D, De Souza L, Marçal E H, De F & Ciuffi K J, *J Environ Chem Eng*, 9 (2021) 105808.
13 Hojiyev R, Ulcay Y & Çelik M S, *Appl Clay Sci*, 146 (2017) 548.
14 Ferreira B F, Ciuffi K J, Nassar E J, Vicente M A, Trujillano, R, Rives V & de Faria E H, *Appl Clay Sci*, 146 (2017) 526.
15 Daitx T S, Carli L N, Crespo J S & Mauler R S, *Appl Clay Sci*, 115 (2015) 157.
16 Khalilzadeh S E, *Colloids Surfaces A: Physicochem Eng Asp*, 598 (2020) 124807.
17 Resende R F, Pereira D H, Papini R M & Magriotis Z M, *Colloids Surfaces A: Physicochem Eng Asp*, 605 (2020) 125340.
18 Marszałek A, Kamińska G & Abdel S N F, *J Water Process Eng*, 46 (2022) 102550.
19 Khodabakhshloo N, Biswas B, Moore F, Du J & Naidu R, *Appl Clay Sci*, 200 (2021) 105883.
20 Dinh V P, Nguyen P T, Tran M C, Luu A T, Hung N Q, Luu T T, Kiet H T, Mai X T, Luong T B, Nguyen T L & Ho H T, *Chemosphere*, 286 (2022) 131766.
21 Yu W H, Ren Q Q, Tong D S, Zhou C H & Wang H, *Appl Clay Sci*, 97 (2014) 222.
22 Wang K, Ma H, Pu S, Yan C, Wang M, Yu J & Zinchenko A, *J Hazard Mater*, 362 (2019) 160.
23 Jia J, *Adsorpt Sci Technol*, 2021 (2021) 1.
24 Li L, Li Y, Cao L & Yang C, *Carbohyd Polym*, 125 (2015) 206.
25 Obi C, Okike U & Okoye P J M C A, *Modern Chem Appl*, 6 (2018) 1.
26 Gilberto T J, Marçal L, Silva J M, Rocha L A, Ciuffi K J, Faria E H & Nassar E J, *J Braz Chem Soc*, 27 (2016) 933.
27 Pires J, Juźków J & Pinto M L, *Colloids Surfaces A: Physicochem Eng Asp*, 544 (2018) 105.
28 Olugbenga A G, Garba M U, Soboyejo W & Chukwu G, *Sci Eng Investigat*, 2 (2013) 1.
29 Shokri E, Yegani R & Ghofrani B J B d l S R d S d L, *Bulletin de la Société Royale des Sciences de Liège*, 86 (2017) 157.
30 Mitra P, Sarkar K & Kundu P P J D S J, *Def Sci J*, 64 (2014) 198.
31 Kausar A, Naeem K, Hussain T, Bhatti H N, Jubeen F, Nazir, A & Iqbal M, *J Mater Res Technol*, 8 (2019) 1161.
32 Zhu L, L Wang & Xu Y, *Appl Clay Sci*, 146 (2017) 35.
33 Arif M, Liu G, Yousaf B, Ahmed R, Irshad S, Ashraf A, Zia-ur-Rehman M, & Rashid M S, *J Clean Prod*, 310 (2021) 127548.
34 Khatamian M, Divband B & Shahi R, *J Water Process Eng*, 31 (2019) 100870.
35 Li Y, Takada H, Shogen A, Saito K, Kobayashi I, Uemura, K & Kanazawa A, *Colloids Surfaces A: Physicochem Eng Asp*, 514 (2017) 126.
36 Halim A A, Halim A A, Aziz H A, Johari M A M & Ariffin K S, *Desalination*, 262 (2010) 31.
37 Beyan S M, Prabhu S V, Sissay T T & Getahun A A, *Bioresour Technol Rep*, 149 (2021) 100664.
38 Akpomie K G & Conradie J, *Sci Rep*, 10 (2020) 14441.
39 Manzar S M, Ahmad T, Ullah N, Chellam P V, John J, Zubair M, Brandão R J, Meili L, Alagha O & Çevik E, *Sep Purif Technol*, 287 (2022) 120559.
40 Gulen B & Demircivi P J J O M S, *J Mol Struct*, 1206 (2020) 127659.
41 Duman O, Özcan C, Polat T G & Tunc S, *Environ Pollut*, 244 (2019) 723.
42 Babas H, Kaichouh G, Khachani M, Karbane M E, Chakir A, Guenbour A, Bellaouchou A, Warad I & Zarrouk A, *Surfaces Interfaces*, 23 (2021) 100962.
43 Shadi A M H, Kamaruddin M A, Niza N M, Omar F M & Hossain M S, *J Environ Chem Eng*, 10 (2022) 107753.
44 Ravi & Pandey L M, *Appl Clay Sci*, 169 (2019) 102.
45 Maged A, Kharbish S, Ismael I S & Bhatnagar A, *Environ Sci Pollut Res*, 27 (2020) 32980.